Discovery of AMP Mimetics that Exhibit High Inhibitory Potency and Specificity for AMP Deaminase

Mark D. Erion,* Srinivas Rao Kasibhatla, Brett C. Bookser, Paul D. van Poelje, M. Rami Reddy, Harry E. Gruber, and James R. Appleman

Contribution from Metabasis Therapeutics, Inc., 9390 Towne Centre Drive, San Diego, California 92121

Received September 2, 1998

Abstract: The first potent, specific, and cell-penetrable AMP deaminase (AMPDA) inhibitors were discovered through an investigation of 3-substituted 3,6,7,8-tetrahydroimidazo[4,5-*d*][1,3]diazepin-8-ol analogues. Inhibition constants for the most potent inhibitors were 10^5-fold lower than the K_M for the substrate AMP. High affinity required the presence of both the 8-hydroxyl and the 3-substituent and is postulated to arise from a cooperative interaction that reduces binding entropy costs and enables the diazepine base to adopt a binding conformation that mimics the transition-state (TS) structure. The high specificity of the inhibitor series for AMPDA relative to other AMP-binding enzymes ($>10^5$) is attributed in part to the diazepine base which favors interactions with residues used to stabilize the TS structure and precludes interactions typically used by AMP-binding enzymes to bind AMP. In contrast, discrimination between AMPDA and adenosine deaminase (ADA), two enzymes postulated to stabilize a similar TS structure, is highly dependent on the 3-substituent. Replacement of the ribose group in the potent ADA inhibitor coformycin (K_i (ADA) $= 10^{-11}$ M vs K_i (AMPDA) $= 3 \times 10^{-6}$ M) with 3-carboxy-4-bromo-5,6,7,8-tetrahydronaphthylethyl led to a $>10^{10}$-fold change in specificity (K_i (ADA) $> 10^{-3}$ M vs K_i (AMPDA) $= 2 \times 10^{-9}$ M). Inhibitors from the series readily penetrate cells and inhibit intracellular AMPDA activity. Incubation of isolated rat hepatocytes with AMPDA inhibitors had no effect on secondary metabolite levels during normoxic conditions but led to increased adenosine production and adenylate sparing under conditions that induce net ATP breakdown. These results suggest that inhibitors of AMPDA may represent site- and event-specific drugs that could prevent or attenuate ischemic tissue damage resulting from a stroke or a heart attack.

Proteins that bind nucleotides represent drug targets with enormous untapped potential. Current targets under investigation within the pharmaceutical industry include P_{2X} and P_{2Y} receptors, which bind nucleotides such as ATP and UTP,[1] GTP-binding proteins,[2] transcription factors, polymerases and other DNA- and RNA-binding proteins, and enzymes within cell-signaling pathways which utilize ATP as a phosphate donor, e.g., tyrosine kinases,[3] cell cycle kinases, and mitogen-activated protein kinase.[4] Other targets include enzymes that control flux through biosynthetic pathways by using nucleotide binding at an allosteric site as an on/off switch. The nucleotide most commonly used for this purpose is AMP since the intracellular AMP level is a good indicator of the cell energy status.[5]

Despite the therapeutic potential of these drug targets, few ligands are known that possess suitable potency, specificity, and bioavailability for clinical development. Discovery of potent and bioavailable ligands is hindered by the hydrophilic nature of nucleotide binding site cavities and the large proportion of the total binding affinity attributed to electrostatic interactions between positively charged amino acid residues and the negatively charged phosphate group. For example, the binding affinity of adenosine for adenylate binding sites is usually 4−6 orders of magnitude less than the affinity of the phosphorylated compound, e.g., ATP or AMP.[6] The dilemma in the design of inhibitors for intracellular enzymes, therefore, stems from the importance of the phosphate or a highly charged phosphate surrogate for binding affinity and the inability of charged molecules to diffuse across cell membranes and penetrate cells. Enzyme specificity also represents a considerable challenge, since many enzyme targets utilize the same ligand. This is especially true for enzymes that bind ATP or AMP, given nature's widespread use of these nucleotides as phosphate donors and allosteric regulators. Consequently, suitable ATP- and AMP-binding site ligands require extraordinarily high ligand specifici-

* To whom correspondence should be addressed. Phone: 619-622-5520. FAX: 619-458-3504. E-mail: erion@mbasis.com.

(1) (a) Jacobson, K. A.; Kim, Y. C.; Wildman, S. S.; Mohanram, A.; Harden, T. K.; Boyer, J. L.; King, B. F.; Burnstock, G. *J. Med. Chem.* **1998**, *41*, 2201−2206. (b) Jianguo, G. G.; MacDermott, A. B. *Nature* **1997**, *389*, 749−753.

(2) Mittal, R.; Ahmadian, M. R.; Goody, R. S.; Wittinghofer, A. *Science* **1996**, *273*, 115−117.

(3) (a) Escalante, C. R.; Yie, L.; Thanos, D.; Aggarwal, A. K. *Nature* **1998**, *391*, 103−106. (b) Levitzki, A.; Gazit, A. *Science* **1995**, *267*, 1782−1788.

(4) (a) Norman, T. C.; Gray, N. S.; Koh, J. T.; Schultz, P. G. *J. Am. Chem. Soc.* **1996**, *118*, 7430−7431. (b) Tong, L.; Pav, S.; White, D. M.; Rogers, S.; Crane, K. M.; Cywin, C. L.; Brown, M. L.; Pargellis, C. A. *Nat. Struct. Biol.* **1997**, *4*, 311−316.

(5) (a) Hardie, D. G. *Nature* **1994**, *370*, 599−600. (b) Corton, J. M.; Gillespie, J. G.; Hardie, D. G. *Curr. Biol.* **1994**, *4*, 315−324. (c) Moore, F.; Weekes, J.; Hardie, D. G. *Eur. J. Biochem.* **1991**, *199*, 691−697.

(6) In addition to having decreased electrostatic interactions, most nucleotide mimetics with decreased negative charge use groups that are structurally dissimilar to phosphate based on geometry, anionic charge, and molecular size. In a few cases, modest binding affinity is retained. For example, a series of cyclic dicarboxylic acids have replaced the phosphate of cyclic guanosine 3′,5′-monophosphate with micromolar inhibitor potencies: Tulshian, D.; Czarniecki, M.; Doll, R. J.; Ahn, H.-S. *J. Med. Chem.* **1993**, *36*, 1210−1220.

10.1021/ja983153j CCC: $18.00
Published on Web 12/31/1998

Scheme 1. Purine Catabolic Pathways

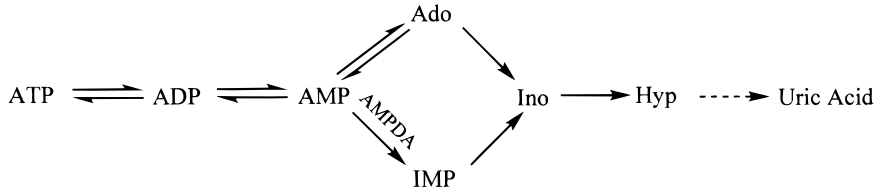

ties or risk generation of dose-limiting toxicities. Unfortunately, discovery of highly specific ligands is hampered by the close similarity of the binding-site architectures of these enzymes as revealed by their X-ray structures.[7]

One well-recognized drug target with promising therapeutic potential is the cytosolic enzyme AMP deaminase (AMPDA, EC 3.5.4.6). AMPDA catalyzes the deamination of AMP to IMP as part of the purine catabolic pathway (Scheme 1).[8] Like many other AMP-binding enzymes, no AMPDA inhibitors have been discovered that simultaneously exhibit high affinity, high specificity, and good cell penetration.[9] Consequently, the physiological role of AMPDA and the therapeutic utility of AMPDA inhibitors are poorly defined. Initial interest in AMPDA as a drug target arose from studies indicating that the human intraerythrocytic malaria parasite, unlike most mammalian cells, lacks the de novo purine biosynthesis pathway and therefore is highly dependent on salvage pathways for the synthesis of purine nucleotides, especially guanylates.[10] Accordingly, AMPDA inhibitors were expected to decrease IMP levels in parasite-infected erythrocytes and thereby inhibit parasite growth by guanylate starvation.

More recently, AMPDA has attracted considerable interest as a potential target for drugs that prevent or limit the tissue damage caused by prolonged ischemic events such as myocardial infarction or stroke.[11] Cells in ischemic tissues naturally attempt to limit cellular damage by breaking down intracellular ATP to adenosine which then diffuses out of the cell and activates nearby membrane receptors. Activation of one or more of the four adenosine receptors (A_1, A_{2A}, A_{2B}, or A_3) leads to a variety of tissue-protective pharmacologies, including vasodilation, decreased oxygen consumption, and decreased inflammation.[12] Inhibitors of AMPDA are expected to further enhance the surge of adenosine production and thereby gain additional pharmacological benefits since a significant portion of the ATP breakdown product and adenosine precursor, AMP, is consumed through deamination to IMP.[13] Little or no elevation of adenosine levels is expected in nonischemic tissues since these tissues are associated with no net ATP breakdown and therefore have low levels of intracellular AMP.[14] The postulated site- and event-specific action of AMPDA inhibitors is of prime importance since earlier attempts to directly stimulate adenosine receptors using nonspecific and receptor subtype-specific agonists consistently failed to produce a successful clinical candidate because of an unacceptably narrow therapeutic index presumably arising from simultaneous stimulation of adenosine receptors in ischemic as well as nonischemic tissues.[12] Evidence supporting AMPDA as an attractive alternative target for cardioprotective drugs is reported in a recent study linking partial AMPDA deficiency to improved prognosis in heart failure patients.[15]

Herein, we describe the first compounds with potencies and specificities sufficient for the delineation of the physiological role of AMPDA and its potential as a drug target.

Inhibitor Design

Transition-state (TS) inhibitors frequently exhibit extraordinarily high binding affinities and enzyme specificities.[16] High affinity is achieved because TS inhibitors engage in the full complement of interactions used by the enzyme during catalysis to preferentially stabilize the TS and thereby lower the reaction energy barrier. High specificity is achieved because the set of interactions used to stabilize a TS are highly dependent on both the specific reaction catalyzed by the enzyme and its unique set of small molecule substrates. Both properties are important in the design of AMPDA inhibitors, since a large enhancement in binding affinity would enable removal of the highly charged phosphate group of AMP and thereby yield compounds that are both cell penetrable and potent inhibitors. TS inhibitors of AMPDA would also exhibit high AMPDA specificity since they differ structurally from the ground-state structure, i.e., AMP, and therefore likely bind with low affinity at other AMP-binding sites.

The TS structure recognized and stabilized by AMPDA is not known in great detail but is expected to resemble the well-characterized TS structure utilized by the related enzyme, adenosine deaminase (ADA),[17] based on the requirement of zinc for efficient catalysis by both enzymes and the similarity in pK_a values and solvent isotope effects.[18] In the case of ADA, deamination is postulated to proceed via the tetrahedral intermediate **1**, which is produced by a rate-limiting, zinc-assisted addition of a hydroxyl ion to C6 of the N1-protonated adenine

(7) For example, see structures of: (a) glycogen phosphorylase b: Sprang, S. R.; Withers, S. G.; Goldsmith, E. J.; Fletterick, R. J.; Madsen, N. B. *Science* **1991**, *254*, 1367−1371. (b) Phosphofructokinase: Schirmer, T.; Evans, P. R. *Nature* **1990**, *343*, 140−145. (c) Fructose 1,6-bisphosphatase: Ke, H.; Liang, J.; Zhang, Y.; Lipscomb, W. N. *Biochemistry* **1991**, *30*, 4412−4420. (d) Adenylate kinase: Schultz, G. E.; Elzinga, M.; Marx. F.; Schirmer, R. H. *Nature* **1974**, *250*, 120−123.

(8) (a) Zielke, C. L.; Suelter, C. H. *J. Biol. Chem.* **1971**, *246*, 1313−1317. (b) Lowenstein, J. M. *Physiol. Rev.* **1972**, *52*, 382−414. (c) Bontemps, F.; Van den Berghe, G.; Hers, H. G. *J. Clin. Invest.* **1986**, *77*, 824−830.

(9) The first AMPDA inhibitors were neither potent nor cell penetrable. Hampton, A.; Sasaki, T.; Perini, F.; Slotin, L. A.; Kappler, F. *J. Med. Chem.* **1976**, *19*, 1029−1033.

(10) (a) Webster, H. K.; Whaun, J. M.; Walker, M. D.; Bean, T. L. *Biochem. Pharmacol.* **1984**, *33*, 1555−1557. (b) Zielke, C. L.; Suelter, C. H. In *The Enzymes*, 3rd ed.; Boyer, P. D., Ed.; Academic Press: New York, 1971; Vol. IV, pp 72−73.

(11) (a) Gruber, H. E. U.S. Patent 4,912,092, 1990. (b) Erion, M. D.; Bookser, B. C., Kasibhatla, S. R. U.S. Patent 5,731,432, 1998.

(12) (a) Jacobson, K. A.; van Galen, P. J. M.; Williams, M. *J. Med. Chem.* **1992**, *35*, 407−422. (b) Erion, M. D. *Annu. Rep. Med. Chem.* **1993**, *28*, 295−304.

(13) (a) Chen, W.; Hoerter, J.; Gueron, M. *J. Mol. Cell. Cardiol.* **1996**, *28*, 2163−2174. (b) Chen, W.; Gueron, M. *J. Mol. Cell. Cardiol.* **1996**, *28*, 2175−2182.

(14) Tagetmeyer, H. *J. Mol. Cell. Cardiol.* **1985**, *17*, 1013−1018.

(15) Loh, E.; Rebbeck, R. R.; Mahoney, P. D.; Stolle, C. A.; Swain, J. L.; Holmes, E. W. *Circulation* **1996**, *94*, (Suppl. 1) 2534.

(16) Wolfenden, R. *Acc. Chem. Res.* **1972**, *5*, 10−18.

(17) (a) Wolfenden, R.; Wentworth, D. F.; Mitchell, G. N. *Biochemistry* **1969**, *16*, 5071−5077. (b) Evans, B. E.; Wolfenden, R. *Biochemistry* **1973**, *12*, 392−397. (c) Kurz, L. C.; Frieden, C. *Biochemistry* **1983**, *22*, 382−389. (d) Kurz, L. C.; Frieden, C. *Biochemistry* **1987**, *26*, 8450−8457. (e) Weiss, P. M.; Cook, P. F.; Hermes, J. D.; Cleland, W. W. *Biochemistry* **1987**, *26*, 6, 7378−7384.

(18) (a) Merkler, D. J.; Schramm, V. L. *Biochemistry* **1993**, *32*, 5792−5799. (b) Merkler, D. J.; Kline, P. C.; Weiss, P.; Schramm, V. L. *Biochemistry* **1993**, *32*, 12993−13001. (c) Bagdassarian, C. K.; Schramm, V. L.; Schwartz, S. D. *J. Am. Chem. Soc.* **1996**, *118*, 8825−8836.

Scheme 2

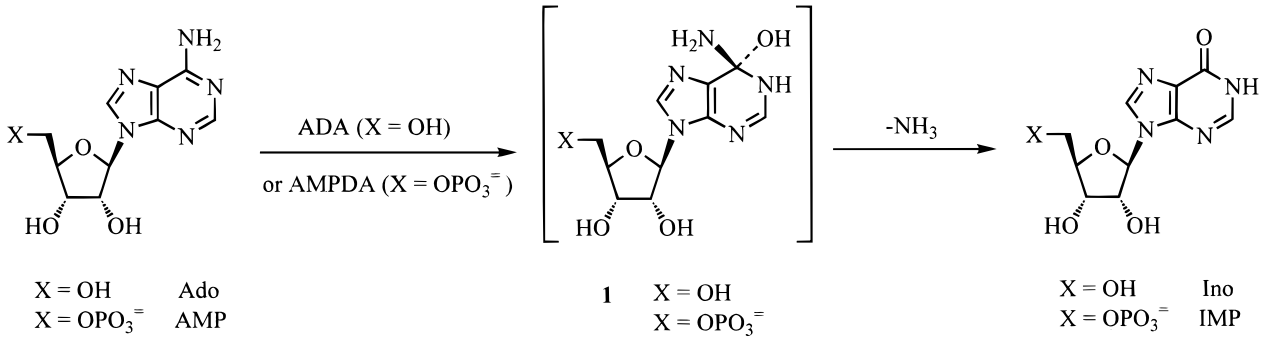

Scheme 3. Hydration of Purine Riboside

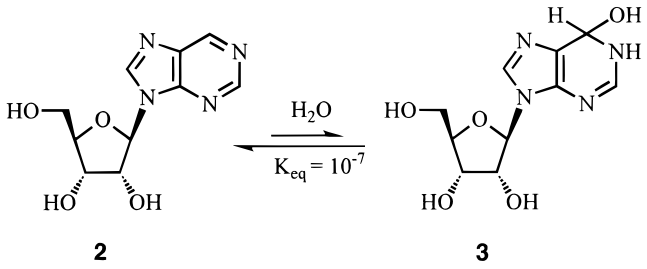

base (Scheme 2). Irreversible breakdown of the intermediate produces the 6-oxo purine product inosine and ammonia. Evidence for the tetrahedral intermediate is derived from pseudosubstrate kinetic data,[17b] inhibitory constants for molecules bearing close resemblance to **1**,[17a] UV-difference[17c] and ^{13}C NMR spectra,[17d] inverse solvent isotope effects,[17e] and more recently, crystallographic data for ADA−inhibitor complexes.[19] Most telling were studies with purine riboside (**2**), which hydrates to an extremely limited extent in aqueous solution ($K_{eq} = 10^{-7}$), but was nevertheless found in the hydrated form (**3**) in the ADA−inhibitor complex (Scheme 3).[19a] The affinity of **3** was estimated to be 10^{-13} M,[20] which presumably reflects its close structural resemblance to the ADA TS structure. The molecular basis for the high affinity is apparent from the X-ray structure of the ADA complex, which shows multiple interactions between the 6-hydroxyl group and both the nearby active-site residues and the zinc ion.

AMPDA is expected to stabilize a similar TS structure on the basis of several findings. First, the aligned sequences for the E-, L-, and M-AMPDA isoenzymes[21] with ADA[22] show that the zinc-binding residues of ADA, namely, His15, His17, His214, and Asp295, and the catalytic residues, namely, His238, Asp296, and Glu217, are completely conserved (Figure 1).[23,18a] Second, ^{14}C and ^{15}N heavy-atom kinetic isotope effects support

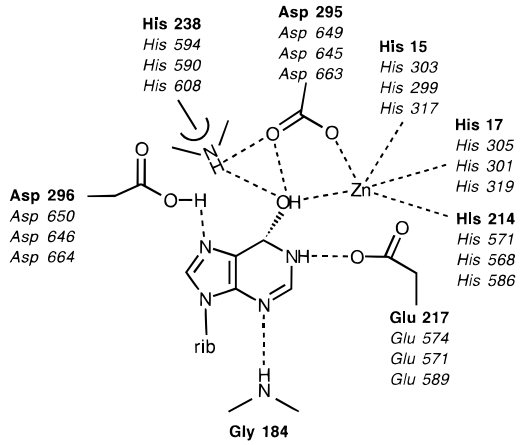

Figure 1. Murine adenosine deaminase interactions with **3** based on the reported X-ray structure.[19] Active-site residues in bold represent residues found in ADA. Residues and associated residue numbers listed underneath represent corresponding residues for the L-, E-, and M-isoenzymes of AMP deaminase, respectively, after sequence alignment.

a short-lived, TS-like, tetrahedral intermediate similar to **1**, generated by addition of a hydroxyl ion to N1-protonated AMP.[18b] Last, the ADA TS inhibitor coformycin (**4**)[24] is a highly potent inhibitor of AMPDA as its corresponding 5′-monophosphate (**5**).[25] Coformycin inhibits human erythrocytic ADA with

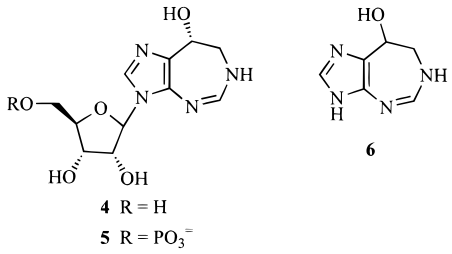

a $K_i = 10$ pM,[24a] whereas coformycin 5′-monophosphate inhibits rabbit muscle AMPDA[25] and yeast AMPDA[26] with K_is of 60 and 10 pM, respectively. Inhibition was postulated to be by TS mimicry since in each case only the 8*R*-hydroxyl stereoisomer exhibited high affinity.[24b,26] In addition to the 8-hydroxyl, the diazepine base and the ribose moieties x were also essential for high ADA affinity with the absence of any one component

(19) (a) Wilson, D. K.; Rudolph, F. B.; Quiocho, F. A. *Science* **1991**, *252*, 1278−1284. (b) Sharff, A. J.; Wilson, D. K.; Chang, Z.; Quiocho, F. A. *J. Mol. Biol.* **1992**, *226*, 917−921. (c) Wilson, D. K.; Quiocho, F. A. *Biochemistry* **1993**, *32*, 1689−1694. (d) Wilson, D. K.; Quiocho, F. A. *Struct. Biol.* **1994**, *1*, 691−694.

(20) (a) Kati, W. M.; Wolfenden, R. *Science* **1989**, *243*, 1591−1593. (b) Kati, W. M.; Wolfenden, R. *Biochemistry* **1989**, *28*, 7919−7927. (c) Jones, W.; Kurz, L. C.; Wolfenden, R. *Biochemistry* **1989**, *28*, 1242−1247. (d) Jones, W.; Wolfenden, R. *J. Am. Chem. Soc.* **1986**, *108*, 7444−7445.

(21) (a) Sabina, R. L.; Morisaki, T.; Clarke, P.; Eddy, R.; Shows, T. B.; Morton, C. C.; Holmes, E. W. *J. Biol. Chem.* **1990**, *265*, 9423−9433. (b) Morisaki, T.; Sabina, R. L.; Holmes, E. W. *J. Biol. Chem.* **1990**, *265*, 11482−11486. (c) Mahnke-Zizelman, D. K.; Sabina, R. L.; *J. Biol. Chem.* **1992**, *267*, 20866−20877.

(22) Yeung, C. Y.; Ingolia, D. E.; Roth, D. B.; Shoemaker, C.; Al-Ubaidi, M. R.; Yen, J. Y.; Ching, C.; Bobonis, C.; Kaufman, R. J.; Kellems, R. E. *J. Biol. Chem.* **1985**, *260*, 10299−10307.

(23) Sequence alignment compared murine ADA with human E-, L-, and M-AMPDA isoenzymes.

(24) (a) Agarwal, R. P.; Spector, T.; Parks, R. E., Jr. *Biochem. Pharmacol.* **1977**, *26*, 359−367. (b) Radzicka, A.; Wolfenden, R. *Methods Enzymol.* **1995**, *249*, 284−312. (c) Bzowska, A.; Lassota, P.; Shugar, D. *Z. Naturforsch.* **1985**, *40c*, 710−714.

(25) Frieden, C.; Kurz, L. C.; Gilbert, H. R. *Biochemistry* **1980**, *19*, 5303−5309.

(26) Merkler, D. J.; Brenowitz, M.; Schramm, V. L. *Biochemistry* **1990**, *29*, 8358−8364.

producing a $>10^6$-fold decrease in potency (e.g., the deribosylated analogue **6**). These results were interpreted as indicating that reduced entropy costs contribute significantly to the high binding affinity.[27]

Two TS inhibitor design strategies were explored during the course of our studies. One strategy focused on purine riboside analogues since the hydrated species of purine riboside (**3**) is thought to gain its extraordinarily high affinity for ADA through TS mimicry and therefore should be readily recognized by the AMPDA purine binding site. The major complication of this approach is that the hydrated form is virtually nonexistent in aqueous solutions ($K_{eq} = 10^{-7}$) which in turn results in the overall modest inhibitory potency associated with **3** ($K_i = 10^{-5}$ M). Accordingly, we focused on the identification of structural modifications of purine riboside that enhance hydration of the 1,6-double bond without compromising the affinity of the hydrated species for the deaminase binding site. Our initial work entailed the development of a method for calculating relative hydration free energies using a combination of quantum mechanical calculations and free energy perturbation methodology[28] and incorporating the results into predictions of the relative binding affinities of ADA inhibitors.[29] The accuracy of these predictions and the similarity of the ADA and AMPDA purine binding sites suggest that a similar strategy could be used in the design of AMPDA inhibitors.

The second strategy, and the subject of this manuscript, entailed the design of coformycin analogues. Coformycin (**4**) is a 50000-fold weaker inhibitor of AMPDA ($K_i = 3\ \mu$M)[30] relative to coformycin monophosphate ($K_i = 0.00006\ \mu$M),[25] which is consistent with the relative affinity decreases observed for other nucleotide-binding enzymes with the corresponding nucleoside analogue. Nevertheless, coformycin represents a good inhibitor of AMPDA and a compound that does not suffer from the limitations of coformycin monophosphate, namely instability to plasma phosphatases and lack of cell membrane permeability. Coformycin itself, however, is not suitable for development as an AMPDA inhibitor because of its high ADA inhibitory potency ($K_i = 10^{-11}$ M) and the strong association between chronic ADA inhibition and severe immunodeficiency.[31] Accordingly, the use of coformycin as a lead TS inhibitor of AMPDA requires modification of the structure in a manner that retains or improves the AMPDA binding affinity while simultaneously reversing the 10^5-fold preference of coformycin for ADA.

Our approach focused on N3-substituted coformycin aglycon analogues since substituents in this region of the active site can clearly discriminate between ADA and AMPDA as illustrated by the $>10^5$-fold difference in specificity exhibited by **4** and **5** (Table 1). Presumably, the large difference in binding affinity arises from the presence of a phosphate binding site in the AMPDA active site which likely contains numerous positively charged residues positioned to accommodate the negatively charged phosphate group, whereas the corresponding residues in the ADA site are hydrophobic. Exploitation of these differences, however, requires the N3-substituent to also maintain optimal alignment of the base or risk compromising the TS mimicry and therefore the high binding affinity.

Table 1. Inhibition Constants

compd	AMPDA K_i (μM)	ADA K_i (μM)	K_i (ADA)/K_i (AMPDA)
4	3	0.00001[a,b]	$\sim 10^{-5}$
5	0.00006[a,c]	>1000[a,d]	$>10^7$
6	>1000	50[e]	$<10^{-1}$
8	4	0.006	$\sim 10^{-3}$
9	45	6.1	10^{-1}
10	0.4	>1000	$>10^3$
13	0.015	>1000	$>10^5$
14	0.002	>1000	$>10^6$
22	>1000		

[a] K_i's determined for the 8*R*-stereoisomer; all other K_i's, except K_i for compound **22**, were determined for the 8*R*/*S* stereoisomeric mixture and therefore are likely to be 2-fold higher than the value for the 8*R*-stereoisomer. [b] Reference 24a. [c] Reference 25. [d] Reference 24c. [e] A value of 40 μM was determined for the 8*R*-stereoisomer, ref 27a.

Scheme 4. General Synthesis of N3-Substituted Coformycin Aglycon Analogues

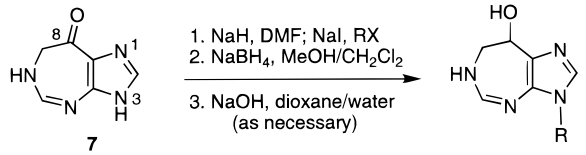

7

Results

N3-substituted coformycin aglycon analogues were synthesized according to the general reaction sequence shown in Scheme 4. Treatment of the known heterocycle 6,7-dihydroimidazo-[4,5-*d*][1,3]diazepin-8(3*H*)-one (**7**),[32] which was prepared in eight steps from 4-methylimidazole, with NaH in DMF followed by the electrophile and NaI gave the N3-alkylation product in modest yield.[33] Reduction of the 8-keto group to the 8-*R*/*S*-alcohol with sodium borohydride followed, when necessary, by treatment with NaOH to hydrolyze the carboxylate ester produced the final product in good overall yield. Two analogues are highlighted here, namely compound **8**, which was prepared

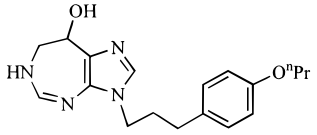

8

using 4-propoxyphenylpropyl methanesulfonate as the electrophile, and compound **10**, which was prepared using 6-mesyloxy-2-benzylhexanoic acid ethyl ester.

Compound **8** inhibited AMPDA and ADA with a K_i of 4 μM and 6 nM, respectively (Table 1). The ADA inhibitory potency represented a 10^4-fold improvement in binding affinity relative to the base alone (**6**) suggesting that the hydrophobic N3-substituent formed highly favorable interactions with the ADA binding site. To assess the binding interactions responsible

(27) (a) Kati, W. M.; Acheson, S. A.; Wolfenden, R. *Biochemistry* **1992**, *31*, 7356−7366. (b) Wolfenden, R.; Wentworth, D. F.; Mitchell, G. N. *Biochemistry* **1977**, *16*, 5071−5077. Similarly, interactions outside of the base binding region were important for cytidine deaminase, see: Carlow, D. C.; Short, S. A.; Wolfenden, R. *Biochemistry* **1998**, *37*, 1199−1203.

(28) Erion, M. D.; Reddy, M. R. *J. Comput. Chem.* **1995**, *12*, 1513−1521.

(29) Erion, M. D.; Reddy, M. R. *J. Am. Chem. Soc.* **1998**, *120*, 3295−3304.

(30) Coformycin (**4**) is reported to inhibit rabbit muscle AMPDA[30a] with $K_i = 50$ nM and yeast AMPDA[30b] with $K_i = 2\ \mu$M. In our studies, the *R*/*S* racemic mixture of **4** inhibited both porcine heart AMPDA and recombinant human *L*-type AMPDA with $K_i = 3\ \mu$M (Table 1). (a) Agarwal, R. P.; Parks, R. E., Jr. *Biochem. Pharmacol.* **1977**, *26*, 663−666. (b) Merkler, D. J.; Schramm, V. L. *J. Biol. Chem.* **1990**, *265*, 4420−4426.

(31) Kredich, N. M.; Hershfield, M. S. In *The Metabolic Basis of Inherited Disease*, 6th ed.; Scrivner, C. R., Eds.; McGraw-Hill: New York, 1989; pp 1045−1075.

(32) Chan, E.; Putt, S. R.; Showalter, H. D. H.; Baker, D. C. *J. Org. Chem.* **1982**, *47*, 3457−3464.

(33) Bookser, B. C.; Kasibhatla, S. R.; Appleman, J. R.; Erion, M. D., unpublished results.

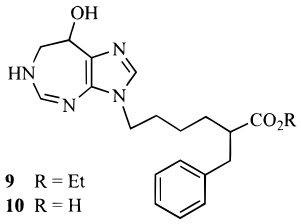

9 R = Et
10 R = H

for the high ADA preference, **8** was evaluated by using the murine ADA X-ray structure[19] and a method for conformation analysis that combines a Monte Carlo searching strategy with energy minimization.[34] The lowest energy conformations showed the N3-substituent to reside in a different region of the binding site cavity than that occupied by the ribose moieties of **3** and **4**. Analysis of the binding interactions depicted in Figure 2 indicated that the low-energy binding conformations were stabilized through van der Waals contacts between the alkylaryl substituent and a hydrophobic cavity produced by the Gly184 α-methylene and the side chains of Met155, Leu106, Leu62, and Ile188 (Leu62 is faint and Ile188 is not shown in Figure 2). In addition, the ether oxygen, which enhances binding affinity 10-fold relative to the corresponding alkyl analogue,[35] formed a hydrogen bond with His157 and a good electrostatic interaction with the main chain NH of Asp185. In contrast, the ribosyl group binds preferentially to the other face of the binding site due presumably to hydrogen bonds formed between the 5′-hydroxyl group and both Asp19 and His17.

Compound **8** also showed an improvement, albeit only 250-fold, over the base **6** in AMPDA inhibitory potency. This gain in potency suggested that, like ADA, the AMPDA binding site has significant hydrophobic character. The larger increase in ADA inhibitory potency, however, indicated that hydrophobic groups at N3 were unlikely to yield compounds with high AMPDA specificity. In contrast, compounds with a negatively charged carboxylate group attached to the hydrophobic N3-substituent at the appropriate position exhibited high AMPDA specificity. For example, compound **10** showed no ADA inhibition even at concentrations of 1 mM. In general, inclusion of a carboxylic acid in the N3-substituent resulted in a 10- to 100-fold increase in AMPDA binding affinity (e.g., **10** vs **9**) and complete specificity for AMPDA.

Synthesis of over 100 other carboxylate-containing compounds led to the discovery of a series of highly potent and selective AMPDA inhibitors containing a 3-carboxy-5,6,7,8-tetrahydronaphthylethyl group at N3.[35] The electrophiles for this series of compounds were synthesized from compound **11**, which was prepared from cyclohexanone in one step by using the procedure reported by Boger and co-workers[36] with some minor modifications (Scheme 5). Conversion of **11** to the desired electrophile **12** was accomplished in two steps and 54% overall yield using a Diels−Alder reaction with dihydrofuran followed by reaction of the crude tricyclic intermediate with BBr_3. Reaction of the electrophile with **7** under the conditions described earlier gave **13**. The brominated analogue **14** was prepared in a similar manner using bromide **19**, which was synthesized by using the route shown in Scheme 5. Intermediate **15** was prepared in one step from **11**, following the reported procedure.[36] Reaction of **15** with Br_2 in acetic acid gave a single brominated product whose structure was assigned as **16** on the basis of NOE experiments. The styryl derivative **17** was prepared via a Stille coupling on the intermediate triflate.[37] Hydroboration of **17** followed by oxidation gave the primary alcohol **18**, which was converted to the bromide **19** with CBr_4 in the presence of PPh_3.

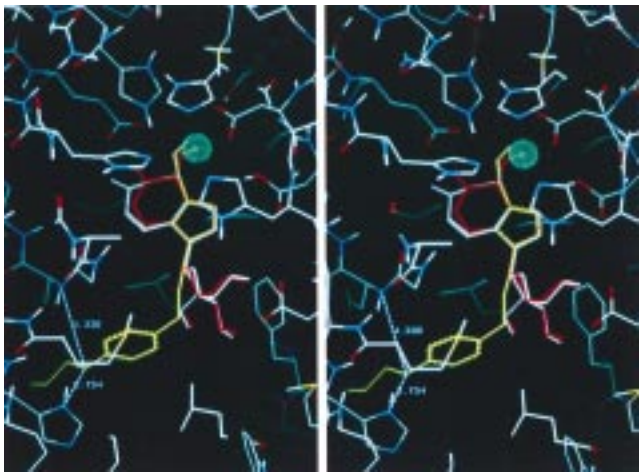

Figure 2. Overlay of purine riboside hydrate (**3**) (red), coformycin (**4**) (white), and compound **8** (yellow) in ADA active site following inhibitor docking and energy minimization (see Experimental Section). Zinc ion is represented by the green sphere. Atomic distances are denoted for the electrostatic interactions between the ether oxygen of **8** and both the imidazole of His157 (2.7 Å) and the backbone amido hydrogen of Asp185 (4.3 Å).

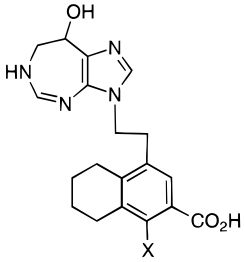

13 X = H
14 X = Br

Compounds **13** and **14** inhibited AMPDA with K_is of 15 and 2 nM, respectively, which represents a 25- to 200-fold improvement in inhibition relative to that by the initial inhibitor **10** (Table 1). No appreciable ADA inhibition was observed at a concentration of 1000 μM. These results indicate that **14** is an AMPDA inhibitor with a potency 1000-fold greater than that of coformycin and only 33-fold lower than that of coformycin monophosphate. Furthermore, the high AMPDA specificity of **14** corresponds to a $>10^{10}$-fold reversal in the AMPDA/ADA specificity relative to that of coformycin.

To assess whether the increased affinities of **13** and **14** were due solely to increased interactions with active-site residues or whether the side chain, like ribose-5-phosphate, resulted in good affinity through a synergistic interaction with the 8-hydroxy tetrahydroimidazol-diazepine base, we prepared the 8-deoxy analogue of **14** (Scheme 6). 4(5)-Nitrohistamine hydrochloride **20**, available from histamine in three steps,[38] was hydrogenated in moderate yield (32%) using triethyl orthoformate to trap the unstable diamine hydrogenation product as the diazepine **21**.

(34) Guida, W. C.; Bohacek, R. S.; Erion, M. D. *J. Comput. Chem.* **1992**, *13*, 214−228.
(35) Kasibhatla, S. R.; Bookser, B. C.; Appleman, J. R.; Probst, G.; Xiao, W.; Erion, M. D., unpublished results.
(36) Boger, D. L.; Mullican, M. D. *Org. Synth.* **1987**, *65*, 98−107.
(37) Echavarren, A. M.; Stille, J. K. *J. Am. Chem. Soc.* **1987**, *109*, 5478−5486.
(38) Tautz, W.; Teitel, S.; Brossi, A. *J. Med. Chem.* **1973**, *16*, 705−707.

Scheme 5[a]

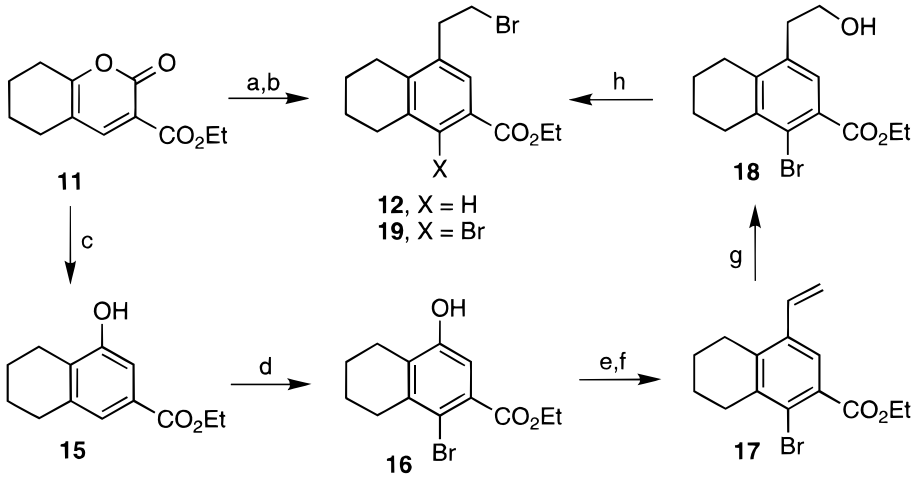

[a] Reagents: (a) **11**,[36] toluene, sealed tube, 140 °C, dihydrofuran. (b) BBr_3, CH_2Cl_2; EtOH, 54% (after two steps). (c) Vinylene carbonate, toluene, sealed tube, see ref 36. (d) Br_2, AcOH. (e) Tf_2O, pyr. (f) $CH_2{=}CHSn(n\text{Bu})_3$, $(PPh_3)_2PdCl_2$, LiCl, DMF. (g) 9-BBN, THF; 30% H_2O_2, 3 N NaOH. (h) CBr_4, PPh_3, CH_2Cl_2.

Scheme 6[a]

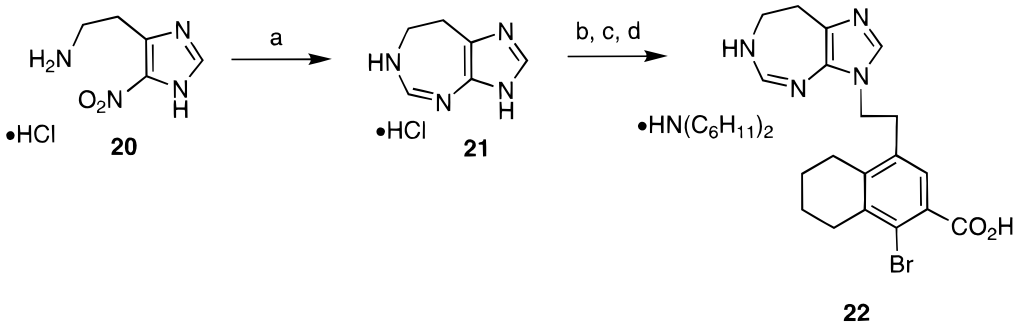

[a] Reagents: (a) **20**,[38] $HC(OMe)_3$, H_2, 10% Pd/C, EtOH. (b) CH_2Cl_2, Et_3N. (c) NaH, DMF, NaI, **23**.[39] (d) 10% Pd/C, H_2 (1 atm), MeOH, $(C_6H_{11})_2NH$.

Alkylation of **21** with the corresponding benzyl ester of **19**, **23**,[39] by using NaH and NaI in DMF provided the N3-alkylation product, which upon hydrogenolysis in the presence of dicyclohexylamine gave **22**.[40] The large decrease in AMPDA inhibitor potency of **22** ($>10^5$-fold) supported the postulate that both the base and the N3-substituent were required for potent inhibition.

The specificity of **13** for the AMP site of AMPDA relative to other AMP binding enzymes was analyzed using five AMP-binding enzymes, namely, adenylate kinase, which uses AMP as a substrate, adenosine kinase, which produces AMP as a product, and glycogen phosphorylase, fructose 1,6-bisphosphatase, and phosphofructokinase, which use AMP as an allosteric regulator. No activity was observed at concentrations >100000-fold the AMPDA K_i.

In addition to being evaluated for potency and specificity, the compound series was evaluated in cell assays to determine the degree of cell penetration and the effect of AMPDA inhibition on intracellular metabolites. Cell uptake studies showed that **13** rapidly distributed across cell membranes and into rabbit erythrocytes to achieve an intracellular concentration 70% of the extracellular concentration in <5 min. Similar results were found by using bovine endothelial cells (~50%) and rat hepatocytes (~100%). Intracellular drug levels were confirmed by analysis of cell lysate AMPDA activity, which closely matched the inhibitory activity predicted from the intracellular drug levels measured by HPLC and the IC_{50} curve for the isolated enzyme.

To assess the functional consequences of AMPDA inhibition, we incubated bovine endothelial cells and isolated rat hepatocytes with **13** and monitored the intracellular levels of key intermediary metabolites. No changes were observed in the levels of ATP, ADP, IMP, or adenosine (Ado), suggesting that flux through AMPDA under basal conditions is minimal. Since flux through AMPDA is expected to increase during net ATP breakdown,[41] we studied isolated rat hepatocytes treated with fructose, which is known to reproducibly produce a dose-dependent decrease in ATP levels as a consequence of the ATP utilization associated with the phosphorylation of fructose by fructose kinase.[42] Similar to results reported in the literature, fructose at a concentration of 0.5 mg/mL in the cell medium depleted cellular ATP levels by 50% in 5−10 min under normal aerobic conditions and elevated downstream metabolites AMP and IMP (Figure 3A). Identically treated cells in the presence of 20 μM **13** exhibited a 33-fold increase in the AMP/IMP ratio, thereby confirming that **13** penetrated the cells and substantially inhibited AMPDA. Ado was elevated 7-fold over baseline levels

(39) The benzyl ester of bromide **19**, compound **23**, was prepared from **18** in three steps. Hydrolysis of **18** with 1 N NaOH in dioxane at 70 °C, followed by alkylation of the carboxylic acid with BnBr in the presence of K_2CO_3 in DMF at room temperature yielded the benzyl ester, which was subsequently treated with CBr_4 in the presence of PPh_3.

(40) ^{1}H NMR showed showed trace amounts of the debrominated product (<5%).

(41) (a) Van den Berghe, G.; Bontemps, M. F.; Van den Berghe, F. *Prog. Neurobiol.* **1992**, *39*, 547−561. (b) Skladanowski, A. C. In *Myocardial Energy Metabolism*; de Jong, J. W., Ed.; Martinus Nijhoff Publishers: Boston, 1988; pp 53−65.

(42) Van den Berghe, G.; Bontemps, F.; Hers, G.-G. *Biochem. J.* **1980**, *188*, 913−920.

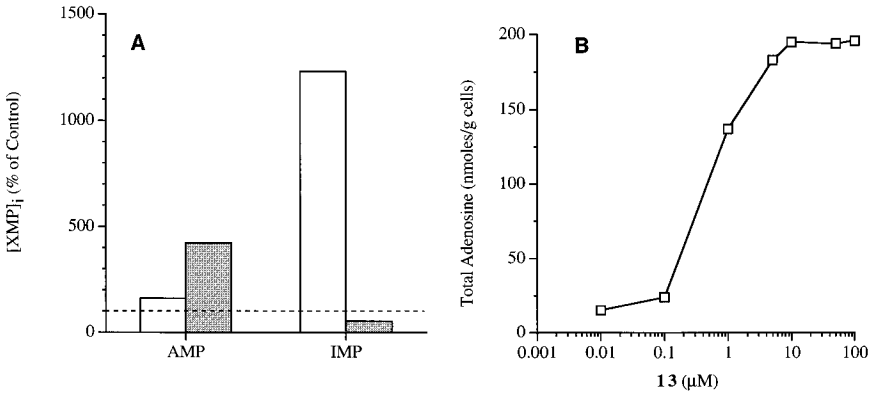

Figure 3. Freshly isolated rat hepatocytes treated with fructose (0.5 mg/mL). (A) AMP and IMP intracellular concentration in hepatocytes preincubated with either vehicle (open bar) or **13** (20 μM) (shaded bar) for 5 min followed by fructose for 5 min relative to non-fructose-treated hepatocytes (control, dashed line). (B) Adenosine concentration vs concentration of **13** at 10 min post-fructose addition. (EC_{50} = 0.4 μM).

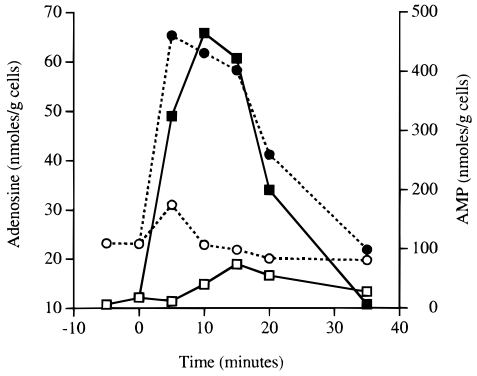

Figure 4. Freshly isolated rat hepatocytes preincubated for 5 min with vehicle or **13** (20 μM) and then treated with fructose (0.5 mg/mL at t = 0 min). AMP (squares, solid lines) and Ado (circles, dashed lines) levels associated with vehicle-treated (open symbols) and drug-treated (shaded symbols) cells were monitored for 35 min.

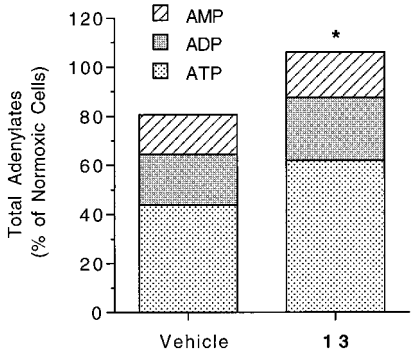

Figure 5. Freshly isolated rat hepatocytes preincubated with vehicle or **13** (20 μM) for 5 min and then subjected to 15 min of anoxia. Figure indicates percent adenylate content relative to t = 0 min. Total adenylate as well as AMP (p = 0.007), ADP (p = 0.017), and ATP (p = 0.003) were significantly elevated relative to adenylate levels in the vehicle-treated cells.

following exposure to fructose, suggesting that AMPDA inhibition had the desired effect of diverting ATP breakdown toward Ado. Most of the Ado (75%) was secreted into the medium as determined in a separate experiment. In addition, the elevation of Ado levels was dose-dependent with an EC_{50} for **13** of 0.4 μM (Figure 3B). Analysis of the time course showed that no changes in AMP or Ado levels occurred during incubation of the cells with **13** prior to the addition of fructose, whereas large increases in both were observed following fructose treatment (Figure 4).

Similar but less pronounced effects were observed in hepatocytes subjected to anoxia rather than fructose treatment. Under anoxic conditions, ATP depletion was slower and less extensive with a 40% reduction observed over 15 min. ADP and AMP levels rose 30% and 160%, respectively. Treatment with **13** (20 μM) led to significantly higher levels of total adenine nucleotides relative to that for vehicle-treated cells and to an adenylate pool equal to that for the normoxic control cells (Figure 5). Consistent with the high degree of adenylate sparing, Ado was elevated a modest 1.2-fold in drug- vs vehicle-treated cells (p = 0.03).

Discussion

Compounds **13** and **14** represent the first potent AMPDA inhibitors described that are not monophosphates. Both compounds also exhibit high enzyme specificity and good cell penetration. Success was achieved using a TS inhibitor strategy as a means to regain a large proportion of the $>10^4$-fold loss in binding affinity associated with removal of the highly charged phosphate group. Evidence supporting these compounds as TS inhibitors is two-fold. First, the 8-deoxy analogue of **14** (compound **22**) exhibited a 10^5-fold decrease in binding affinity, which is consistent with the loss in potency observed in earlier studies with the 8*S*-stereoisomer of 2′-deoxycoformycin and ADA[24b] and the 8*S*-isomer of coformycin monophosphate and AMPDA.[26] In the case of ADA, the large contribution of a single hydroxyl group is attributed to its interactions with the active-site zinc ion and nearby residues.[19] Since the residues used by ADA to coordinate the zinc ion and bind the TS inhibitor **3** are completely conserved in the three AMPDA isoenzymes, the large decrease in inhibitory potency for **22** suggests that the 8-hydroxyl of **14** forms the same hydrogen bond pattern and is in a position suitable for TS mimicry.

A second observation indicating that the inhibitor series achieves high potency through TS mimicry is the poor AMPDA inhibitory potency of the base, i.e., **6**, and therefore the high dependence of inhibition on the N3-substituent. A similar finding was reported for ADA by Wolfenden in that the ribose group of coformycin proved to be essential for high affinity presumably because it reduced entropy losses through assisting the alignment of the base and the 8-hydroxyl group in a manner most optimal for TS mimicry.[27a] Analysis of coformycin monophosphate (**5**) binding to AMPDA shows a similar dependency since removal of the ribose 5-phosphate group led to a 10^8-fold loss in binding affinity. Not all of the lost binding affinity is attributed to decreased TS mimicry since some of the decreased affinity is associated with removal of the phosphate group ($\sim 10^4$) which is likely to be reflected in both the ground state and TS.

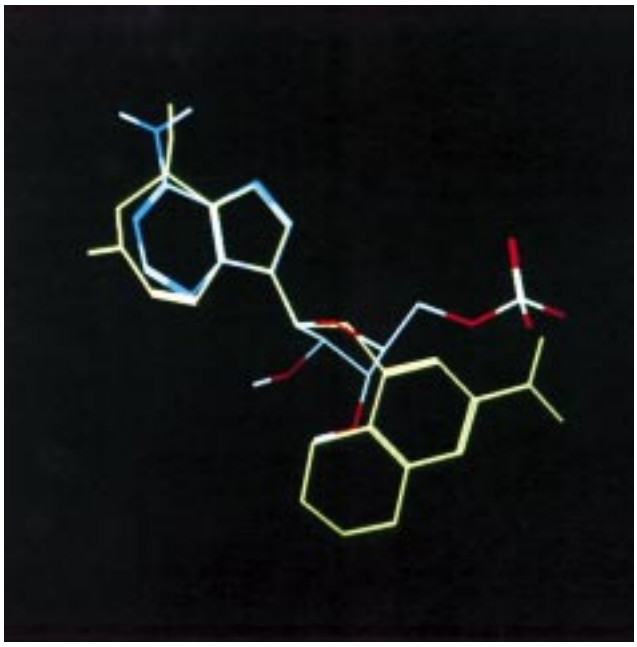

Figure 6. Structure overlay of AMP and compound **13** (yellow). The AMP structure is derived from the Cambridge crystal structure database (FEXROP, $r = 0.0580$). Compound **13** represents the energy-minimized structure (3.2 kcal/mol above the global minimum) most closely matching the structure of AMP.

Discovery of compounds with N3-substituents that retain most of the potency of coformycin monophosphate suggests that groups other than ribose 5-phosphate can position the diazepine base in a manner analogous to the TS structure and thereby gain the synergistic effect of the base and N3-substituent. The modest 17-fold decrease in potency (assumes only the 8*R*-stereoisomer is active) of **14** relative to coformycin monophosphate (**5**) is remarkable, given that the substituent not only had to maintain good TS mimicry but also had to regain the binding energy associated with the phosphate moiety. In general, carboxylic acids are considered relatively poor mimics of phosphates, given the large difference in geometry (planar vs tetrahedral), molecular charge, and number of heteroatoms. Some gain in affinity is possible with a carboxylic acid, however, if the carboxylic acid is positioned near the positively charged phosphate binding site. In this case, favorable through-space electrostatic interactions are possible as was concluded in earlier studies with purine nucleoside phosphorylase and a carboxylic acid-containing inhibitor.[43] The possibility that the carboxylate increases binding affinity 10−100 fold[33,35] through interaction with the phosphate binding site is supported by the finding that low-energy conformations of **13** position the carboxylate in the same region of conformational space as that of the phosphate group of AMP (Figure 6).

In addition to inhibitory potency, the diazepine base and N3-substituent were also essential for the high specificity of the inhibitor series for AMPDA relative to other AMP-binding enzymes and adenosine deaminase. Crystallographic studies indicate that AMP-binding enzymes utilize very similar binding site cavities and interactions to bind AMP. One feature common to nearly all AMP binding sites is the presence of a hydrogen bond-donating residue near N1 and two hydrogen bond-accepting residues near the 6-amino group. Recently published protein engineering studies suggest that this hydrogen bond pattern accounts for the high binding affinity and specificity of these enzymes for adenine-containing ligands (e.g., AMP) relative to the corresponding 6-oxopurine analogues (e.g., GMP).[44] Consistent with these reports was our finding that the TS inhibitor **13** showed no appreciable binding to five other AMP-binding enzymes. The molecular basis for the high selectivity is suggested by the ADA-**3** X-ray structure which showed the 6-hydroxyl of **3** to form strong interactions with active-site residues out of the plane of the base. In contrast, AMP binding sites typically interact with the 6-amino group through in-plane interactions and therefore contain residues poorly positioned to interact with the 8-hydroxyl of coformycin analogues. Furthermore, like **3**, coformycin has a hydrogen bond donor near the corresponding N1 position of adenine that likely donates a hydrogen bond to the nearby negatively charged Glu217, whereas most other AMP binding sites utilize the opposite hydrogen bond pattern.

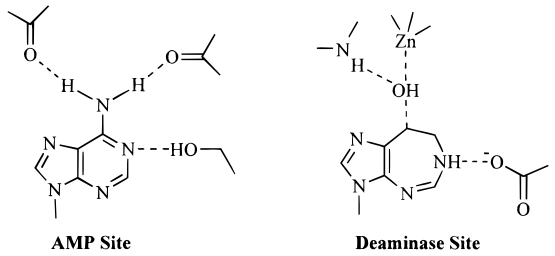

The high specificity of the inhibitor series for AMPDA over ADA was dependent on the N3-substituent rather than the diazepine base since the residues used by ADA to bind the base were completely conserved in AMPDA. Hydrophobic N3-substituents led to compounds with deaminase specificities that favored ADA by as much as 1000-fold and potencies in the low nanomolar range (e.g., **8**, $K_i = 6$ nM). In contrast, analogues with hydrophobic N3-substituents containing a carboxylic acid achieved extraordinarily high AMPDA specificities. Since the carboxylic acid provided only a modest gain in AMPDA inhibitory potency, the large increase in specificity arises predominantly from the inability of the ADA binding site to accommodate a negatively charged group. Consistent with this conclusion are molecular modeling studies showing that inhibitors containing a carboxylic acid had much lower interaction energies than the corresponding descarboxy analogues. Experimentally, compounds **13** and **14** favored AMPDA binding by at least 10^5-fold on the basis of the ratio K_i(ADA)/K_i(AMPDA). Thus, replacement of the ribosyl moiety of coformycin with the 3-carboxytetrahydronaphthylethyl group led to a 10^{10}-fold change in deaminase specificity.

In addition to high AMPDA binding affinity and enzyme specificity, the compound series showed good cell penetration. Analysis of intracellular inhibitor concentration over time by HPLC showed that compound **13** rapidly equilibrated across cell membranes (≤5 min) to achieve an intracellular concentration approximately 50% of the extracellular concentration. The intracellular inhibitor concentration was confirmed by determining AMPDA activity in cell lysates and showing that the degree of AMPDA inhibition closely corresponded to the inhibition

(43) (a) Erion, M. D.; Niwas, S.; Rose, J. D.; Ananthan, S.; Allen, M.; Secrist, J. A., III; Babu, Y. S.; Bugg, C. E.; Guida, W. C.; Ealick, S. E.; Montgomery, J. A. *J. Med. Chem.* **1993**, *36*, 3771−3783. (b) Ealick, S. E.; Babu, Y. S.; Bugg, C. S.; Erion, M. D.; Guida, W. C.; Montgomery J. A.; Secrist, J. A., III. *Proc. Natl. Acad. Sci. U.S.A.* **1991**, *88*, 11540−11544.

(44) (a) Erion, M. D.; Takabayshi, K.; Smith, H. B.; Kessi, J.; Wagner, S.; Honig, S.; Shames, S. L.; Ealick, S. E. *Biochemistry* **1997**, *36*, 11725−11734. (b) Erion, M. D.; Guida, W. C.; Stoeckler, J. D.; Ealick, S. E. *Biochemistry* **1997**, *36*, 11735−11748. (c) Stoeckler, J. D.; Poirot, A. F.; Smith, R. M.; Parks, R. E., Jr.; Ealick, S. E.; Takabayashi, K.; Erion, M. D. *Biochemistry* **1997**, *36*, 11749−11756.

expected for that inhibitor concentration with the isolated enzyme. Last, endothelial cells treated with hydrophobic proesters of **13**[35] showed intracellular levels of **13** similar to those for nonproester treated cells, indicating that the generation of **13** intracellularly through the action of esterases did not result in a trapping and accumulation of **13** inside the cell. These studies therefore suggest that **13** enters cells, most likely via passive diffusion, and that the levels achieved are relatively high despite the presence of a carboxylic acid and a log $P \approx -0.7$. Previous studies with other carboxylic acids (e.g., NSAIDs, purine nucleoside phosphorylase inhibitors,[43a] angiotensin converting enzyme inhibitors, etc.) suggest that carboxylic acids exhibit good cell penetration properties relative to phosphonic acids but are less cell penetrable than highly lipophilic compounds.

Inhibition of AMPDA in Cells

Extracellular adenosine concentration is tightly regulated in vivo by enzymes controlling adenosine metabolism and production. Adenosine production is highly dependent on ATP breakdown and the resulting increase in intracellular AMP levels as well as the enzymes that utilize AMP, namely 5′-nucleotidase, which catalyzes the dephosphorylation of AMP to adenosine, and AMPDA, which catalyzes the deamination of AMP and thereby effectively limits adenosine production by diverting AMP metabolism toward IMP. At the start of our work, flux through both enzymes was expected to dramatically increase during hypoxia on the basis of the increase in AMP concentration ($\sim$1 μM to 1 mM) and the relatively high K_M's of both enzymes for AMP. Unknown, however, was the proportion of AMP breakdown catalyzed by AMPDA and therefore the maximal increase in adenosine production expected for an AMPDA inhibitor.[13]

To assess the effect of AMPDA inhibition on secondary metabolite levels during normoxic conditions and during conditions that result in net ATP breakdown, we analyzed freshly isolated rat hepatocytes treated with an AMPDA inhibitor and subjected to either vehicle, fructose, or anoxia. Fructose alone induced approximately 50% ATP breakdown over a 10 min period and elevations in the levels of the downstream metabolites AMP, IMP, and Ado of 4.7-, 6- and 2-fold, respectively. In the presence of **13** (20 μM), the metabolite profile changed dramatically as indicated by the 33-fold increase in the AMP/IMP ratio and the 7-fold rise in total adenosine. Importantly, AMPDA inhibition had no effect on either AMP or adenosine levels in the absence of fructose. These results suggest that AMPDA inhibitors might elevate adenosine levels with high event specificity and therefore enhance local adenosine levels only at ischemic sites and not in nonischemic tissues. Accordingly, AMPDA inhibitors might raise adenosine in a manner that provides pharmacological benefit to the ischemic tissue while minimizing side effects and unrelated pharmacology.

Another possible benefit of AMPDA inhibition is apparent from the results obtained with hepatocytes subjected to anoxia. Similar to fructose, anoxia led to ATP breakdown, an elevation of AMP levels (160%) and, albeit less pronounced, an elevation of adenosine levels. In contrast to results obtained with fructose, cells subjected to anoxia in the presence of **13** showed only a slight further enhancement of adenosine levels. Instead, there was a significant increase in the adenylate pool with total adenylates (ATP + ADP + AMP) achieving a level equal to normoxic cells. These results suggest that the AMP preserved through AMPDA inhibition is predominantly reconverted to ADP and ATP by adenylate kinase and not to adenosine. The reason for the difference in the metabolic fate of AMP under anoxic conditions relative to fructose treatment is unclear but may relate to differences in adenosine kinase activity (unpublished results). This adenylate sparing activity suggests that AMPDA inhibition might prevent the tissue damage associated with conditions such as acute myocardial infarction, stroke, and heart failure all of which involve net ATP breakdown, decreased adenylate pools, and irreversible tissue damage.[45] Agents that prevent loss of the adenylate pool may therefore increase the probability of tissue survival after reperfusion since the adenylates can serve to assist in the repletion of ATP reserves following reoxygenation of the tissue. Recent studies in heart failure patients indicate that partial AMPDA deficiency is associated with improved prognosis based on the observation that these patients tolerate a longer duration of heart failure symptoms before referral for transplant evaluation than patients with normal AMPDA levels.[15]

Concluding Remarks

Despite nearly two decades of pharmaceutical research and impressive pharmacological activity in numerous animal models of human diseases, no adenosine receptor agonist, with the exception of adenosine itself, has successfully completed human clinical trials. The lack of success is attributed to the simultaneous activation of adenosine receptors at sites unrelated to the disease and thereby the production of dose-limiting side effects and an overall narrow therapeutic window.[12,46] As presented in this paper, AMPDA inhibitors represent an alternative strategy for activation of adenosine receptors. Our discovery and characterization of the first potent, specific, and cell penetrable inhibitor of AMPDA led to the observation that AMPDA inhibitors elevate adenosine levels only in cells undergoing net ATP breakdown. Accordingly, AMPDA inhibitors are expected to elevate adenosine levels in the whole animal only at sites undergoing an ischemic episode and thereby protect tissues from ischemic damage incurred during a stroke, heart attack, or related conditions without simultaneously producing adenosine-mediated side effects.

Experimental Section

General Procedures. Glassware for moisture-sensitive reactions was flame-dried and cooled to rt in a desiccator. All reactions were carried out under an atmosphere of nitrogen. Anhydrous solvents were purchased from Aldrich and stored over 4 Å molecular sieves. THF was freshly distilled from Na/benzophenone ketyl under nitrogen. Flash chromatography was performed on 230−400 mesh EM Science silica gel 60. Melting points were determined in open capillary tubes with a Thomas-Hoover capillary melting point apparatus and are uncorrected. ^{1}H and ^{13}C NMR were obtained on a Varian Gemini-200 operating at 200 and 50 MHz, respectively. ^{1}H and ^{13}C NMR spectra were recorded in units δ with tetramethylsilane (δ 0.00) and $CDCl_3$ (δ 77.0) or DMSO-d_6 (δ 39.9) as reference line internal standards, respectively. UV spectra (200−350 nm) of methanolic solutions were recorded on a Kontron Uvikon 860. Microanalyses were carried out at Robertson Laboratory, Inc. Madison, NJ.

3,6,7,8-Tetrahydroimidazo[4,5-*d*][1,3]diazepin-8-ol (6).[47] A mixture of ketone **7** (150 mg, 1 mmol) and $NaBH_4$ (40 mg, 1 mmol) in 5

(45) (a) Ingwall, J. S. *Circulation* **1993**, *87*, (Suppl. VII), 58−62. (b) Nascimben, L.; Friedrich, J.; Liao, R.; Pauletto, P.; Pessina, A.; Ingwall, J. S. *Circulation* **1995**, *91*, 1824−1833. (c) Scheuer, J. *Circulation* **1993**, *87*, (Suppl. VII), 54−57.

(46) (a) Appleman, J. R.; Erion, M. D. *Expert Opin. Invest. Drugs* **1998**, *7*, 225−243. (b) Williams, M. *Drug Dev. Res.* **1993**, *28*, 438−444.

(47) The 8*R*-coformycin aglycon analogue was prepared previously with minimal characterization: (a) Smal, E., Ph.D. Thesis, University of Alabama, 1985. (b) Al-Razzak, L. A.; Bendetti, A. E.; Waugh, W. N.; Stella, V. J. *Pharm. Res.* **1990**, *7*, 452.

mL of CH_2Cl_2 and 5 mL of methanol was stirred at rt for 1 h and then slurried with 2 g of SiO_2. The solvent was evaporated and the powder loaded onto a SiO_2 column and eluted with CH_3CN/EtOH/NEt_3 mixtures of 10:1:0.1, 5:1:0.06, 3:1:0.04, and 1:1:0.02 to yield 111 mg (73%) of **6** as a brown solid (deliquescent and blackened on standing in air): mp 124−127 °C; R_f 0.23 (3:1 CH_3CN/0.2 M NH_4Cl); UV (MeOH) 205 nm (ϵ 15700), 283 (9060); ^{1}H NMR (DMSO-d_6) δ 3.24 (s, 2H), 4.84 (br s, 1H), 5.23 (br s, 1H), 7.18 (br s, 1H), 7.30 (s, 1H), 8.06 (br s, 1H), 11.93 (br s, 1H); ^{13}C NMR (DMSO-d_6) δ 47.9 (C-7), 65.9 (C-8), 127.3 (C-8a), 129.9 (C-5), 136.9 (C-3a), 146.6 (C-2); MS (ES) *m*/*z* 153 ([M + H]$^+$), 151 ([M − H]$^-$). An analytical sample was prepared by adding a small amount of ethanolic HCl to a methanolic (5 mL) solution of **6** (53 mg). The solvent was evaporated and the residue triturated with hot MeOH. The resulting white solid was dried under high vacuum to provide 31 mg of the HCl salt of **6** (deliquescent and blackened on standing in air): mp 214 °C (dec); ^{1}H NMR (DMSO-d_6) δ 3.47 (dd, 1H, J = 12, 5 Hz), 3.60 (br d, 1H, J = 12 Hz), 5.02 (dd, 1H, J = 5, 2 Hz), 7.65 (s, 1H), 7.95 (d, 1H, J = 7 Hz). Anal. Calcd for $C_6H_8N_4$·HCl·0.33H_2O: C, 37.04; H, 5.00; N, 28.80. Found: C, 37.51; H, 5.07; N, 28.13.

6,7-Dihydroimidazo[4,5-*d*][1,3]diazepin-8(3*H*)-one (7). A suspension of 10 g of 6,7-dihydroimidazo-[4,5-*d*][1,3]diazepin-8(3*H*)-one hydrochloride DMSO solvate[32] in 50 mL of triethylamine was stirred for 30 min before adding 500 mL of CH_2Cl_2. The mixture was then stirred for 10 min and filtered. The solid was collected and washed with CH_2Cl_2 to provide 5.65 g (91%) of **7** as a light brown solid: mp 260 °C; ^{1}H NMR (DMSO-d_6) δ 3.79 (br s, 2H), 7.33 (s, 1H), 7.63 (br s, 1H), 8.3 (br s, 1H), 12.2 (br s, 1H); ^{13}C NMR (DMSO-d_6) δ 52.8 (C-7), 115.4 (C-8a), 136.2 (C-5), 149.6 (C-2), 161.1 (C-3a), 180.2 (C-8). Anal. Calcd for $C_6H_6N_4O$·0.33H_2O: C, 46.17; H, 4.30; N, 35.89. Found: C, 46.32; H, 4.08; N, 35.76.

3-(3-(4-Propoxyphenyl)propyl)coformycin Aglycon (8). Prepared from 4-propoxyphenylpropyl methanesulfonate and ketone **7** as described for the preparation of compound **9**: mp 134−135 °C; ^{1}H NMR (DMSO-d_6) δ 0.96 (t, 3H, J = 7 Hz), 1.71 (hex, 2H, J = 7 Hz), 1.93 (quin, 2H, J = 7 Hz), 2.49 (t, 2H, J = 7 Hz), 3.16 (br s, 2H), 3.84 (t, 2H, J = 7 Hz), 3.88 (t, 2H, J = 7 Hz), 4.62 (br s, 1H), 4.90 (d, 1H, J = 5 Hz), 6.83 (d, 2H, J = 8 Hz), 6.96 (d, 1H, J = 4 Hz), 7.10 (d, 2H, J = 8 Hz), 7.29 (s, 1H), 7.4−7.5 (m, 1H). Anal. Calcd for $C_{18}H_{24}N_4O_2$: C, 65.83; H, 7.37; N, 17.06. Found: C, 65.49; H, 6.99; N, 16.81.

3-(5-Carboethoxy-6-phenylhexyl)coformycin Aglycon (9). Sodium hydride (479 mg of a 60% oil dispersion, 12 mmol) was washed with hexanes, suspended in DMF (55 mL), and treated with ketone **7** (1.71 g, 11.4 mmol). The mixture was heated to 60 °C for 30 min under N_2, cooled to 22 °C, and treated with a solution of ethyl 2-(benzyl)-6-methanesulfonyloxyhexanoate (3.74 g, 11.4 mmol) in 12 mL of DMF. NaI (427 mg, 2.85 mmol) was then added and the resulting mixture stirred at 90 °C for 90 min to produce a homogeneous brown solution. The solvent was removed and the residue chromatographed on 220 g of SiO_2. Elution with CH_2Cl_2/methanol mixtures of 20:1, 18:1, and 16:1 provided 1.44 g (33%) of 3-(5-carboethoxy-6-phenylhexyl)-6,7-dihydroimidazo[4,5-*d*]-[1,3]diazepin-8(3*H*)-one as a light yellow gum: ^{1}H NMR (DMSO-d_6) δ 1.01 (t, 3H, J = 7 Hz), 1.20 (quin, 2H, J = 7 Hz), 1.4−1.8 (m, 4H), 2.62 (m, 1H), 2.7−2.8 (m, 2H), 3.73 (d, 2H, J = 4 Hz), 3.92 (t, 2H, J = 7 Hz), 3.94 (q, 2H, J = 7 Hz), 7.1−7.3 (m, 5H), 7.40 (d, 1H, J = 4 Hz), 7.61 (s, 1H), 8.35 (br m, 1H).

The ketone (1.43 g, 3.75 mmol) in CH_2Cl_2/MeOH (1:1, 36 mL) was treated with $NaBH_4$ (146 mg, 3.75 mmol). After stirring the mixture at rt for 45 min, SiO_2 (4.5 g) was added and the solvent evaporated. The powder was loaded onto a 45 g SiO_2 column and eluted with CH_2Cl_2/methanol/triethylamine mixtures of 25:1:0.25 and 20:1:0.2. The fraction containing the product was reduced to a minimal volume and diluted with ether to yield after filtration and drying 1.07 g (74%) of compound **9** as a white solid: mp 121−124 °C; ^{1}H NMR (DMSO-d_6) δ 1.03 (t, 3H, J = 7 Hz), 1.22 (q, 2H, J = 7 Hz), 1.4−1.7 (m, 4H), 2.5−2.7 (m, 1H), 2.7−2.8 (m, 2H), 3.15 (m, 2H), 3.81 (t, 2H, J = 7 Hz), 3.95 (q, 2H, J = 7 Hz), 4.81 (m, 1H), 4.91 (d, 1H, J = 5 Hz), 6.95 (d, 1H, J = 4 Hz), 7.1−7.3 (m, 5H), 7.25 (s, 1H), 7.45 (m, 1H). Anal. Calcd for $C_{21}H_{28}N_4O_3$: C, 65.60; H, 7.34; N, 14.57. Found: C, 65.39; H, 7.34; N, 14.52.

3-(5-Carboxy-6-phenylhexyl)coformycin Aglycon (10). The ester **9** (4.13 g, 10.7 mmol) was dissolved in 60 mL of dioxane and treated with 0.25 M NaOH (64 mL, 16 mmol). The mixture was stirred at 55 °C for 14 h, cooled, diluted with 20 mL of water, and extracted with CH_2Cl_2. The aqueous layer was slurried with Dowex-1 acetate (ca. 25 mL volume) for 1 h and then filtered. The resin was washed with water and then batchwise slurried with 0.1 N AcOH (6 × 100 mL) for 20 min each at 5 °C. After filtration, the combined filtrates were frozen and lyophilized to provide 2.9 g (70%) of the carboxylate **10** as a white solid: mp 58−61 °C; R_f 0.39 (3:1 CH_3CN/0.2 N NH_4Cl); ^{1}H NMR (DMSO-d_6) δ 1.1−1.7 (m, 6H), 2.6−2.9 (m, 3H), 3.15 (br s, 2H), 3.81 (t, 2H, J = 7 Hz), 4.80 (br s, 1H), 6.96 (d, 1H, J = 4 Hz), 7.1−7.3 (m, 5H), 7.19 (s, 1H), 7.47 (m, 1H). Anal. Calcd for $C_{19}H_{24}N_4O_3$·0.2CH_3CO_2H·1H_2O: C, 60.26; H, 6.99; N, 14.48. Found: C, 60.21; H, 6.80; N, 14.33.

Ethyl 1-(2-Bromoethyl)-5,6,7,8-tetrahydronaphthyl-3-carboxylate (12). A solution of ethyl 2-oxo-5,6,7,8-tetrahydro-2H-1-benzopyran-3-carboxylate **11**[36] (20.0 g, 0.09 mol) and distilled 2,3-dihydrofuran (63.0 g, 0.9 mmol) in a dry 18 × 4 cm resealable glass tube was flushed with Ar and sealed with a Teflon plug. The reaction was heated at 140 °C for 14 h. The resulting dark reaction mixture was then cooled and the excess 2,3-dihydrofuran evaporated under reduced pressure to afford 22.9 g of a dark residue presumed to be the tricyclic Diels−Alder adduct: ^{1}H NMR ($CDCl_3$) δ 1.28 (t, 3H, J = 7.7 Hz), 1.3−3.0 (series of m, 10H), 3.6 (m, 2H), 4.2 (m, 3H), 4.7 (d, 1H, J = 9.4 Hz), 6.9 (s, 1H). The crude product was dissolved in 200 mL of CH_2Cl_2, cooled to −78 °C, and treated with BBr_3 (67.6 g, 0.27 mol). The reaction mixture was then warmed slowly to rt, stirred 4 h, cooled again to −78 °C, and quenched with 60 mL of EtOH. After the mixture stirred 16 h, the solvent was evaporated, and the residue was diluted with hexane, washed with water and 10% bicarbonate, and dried ($MgSO_4$). The solvent was removed and the residue purified by chromatography (2% EtOAc in hexane) to give 15.1 g (54%) of **12** as an oil: ^{1}H NMR (DMSO-d_6) δ 1.3 (t, 3H, J = 7 Hz), 1.7 (m, 4H), 2.7 (m, 4H), 3.1 (t, 2H, J = 7 Hz), 3.68 (t, 2H, J = 7 Hz), 4.32 (q, 2H, J = 7 Hz), 7.56 (s, 1H), 7.62 (s, 1H).

3-[2-(3-Carboxy-5,6,7,8-tetrahydronaphthyl)ethyl]coformycin Aglycon (13). 13 was prepared from compound **12** and ketone **7** by using the procedures described for the preparation of compounds **9** and **10**: mp >220 °C dec; UV (MeOH) 214 nm (ϵ 29700), 243 (12400), 282 (8190); ^{1}H NMR (DMSO-d_6) δ 1.74 (m, 4H), 2.77 (m, 4H), 2.9 (t, 2H, J = 7 Hz), 3.1 (br s, 2H), 4.1 (t, 2H, J = 7 Hz), 4.8 (br s, 1H), 7.0 (d, J = 4 Hz, 1H), 7.3 (s, 1H), 7.5 (br s, 3H). Anal. Calcd for $C_{19}H_{22}N_4O_3$·0.5H_2O·0.3CH_3CO_2H: C, 61.71; H, 6.39; N, 14.68. Found: C, 61.32; H, 6.23; N, 14.55.

Ethyl 1-Hydroxy-4-bromo-5,6,7,8-tetrahydronaphthyl-3-carboxylate (16). To a solution of **15**[36] (3.2 g, 14.5 mmol) in acetic acid (30 mL) was added a solution of bromine (0.75 mL, 14.5 mmol) in acetic acid (30 mL) over 1.5 h. After an additional 1 h, the solvent was evaporated, and the residue was diluted with ice−water, extracted with ether, dried ($MgSO_4$), and purified on SiO_2 (30% EtOAc/hexane) to give 3.0 g (69%) of **16**: ^{1}H NMR (DMSO-d_6) δ 1.30 (t, 3H, J = 7 Hz), 1.7 (m, 4H), 2.6 (m, 4H), 4.30 (q, 2H, J = 7 Hz), 6.9 (s, 1H), 9.9 (s, 1H).

Ethyl 1-Vinyl-4-bromo-5,6,7,8-tetrahydronaphthyl-3-carboxylate (17). A solution of **16** (2.0 g, 6.7 mmol) in pyridine (15 mL) was cooled to 0 °C and slowly treated with trifluoromethanesulfonic anhydride (1.35 mL, 8.05 mmol). After warming to rt, the mixture was stirred for 3 h and the solvent evaporated. The residue was diluted with 100 mL of ice−water and extracted with ether. The combined extracts were dried ($MgSO_4$) and evaporated to afford 2.4 g of a brown syrup. The crude triflate was dissolved in DMF (30 mL), treated with $(PPh_3)_2PdCl_2$ (0.2 g, 0.33 mmol), LiCl (0.85 g, 20.1 mmol), and vinyltributyltin (2.35 mL, 8.05 mmol), and heated at 80 °C. After 4 h, the solvent was evaporated, and the residue was diluted with ether, washed with water and saturated NaF, dried ($MgSO_4$), and purified by chromatography (5% EtOAc in hexane) to give 1.6 g (77%) of **17**: ^{1}H NMR (DMSO-d_6) δ 1.33 (t, 3H, J = 7 Hz), 1.7 (m, 4H), 2.7 (m, 4H), 4.32 (q, 2H, J = 7 Hz), 5.3−5.8 (m, 2H), 6.8−7.0 (m, 1H), 7.5 (s, 1H).

Ethyl 1-(2-Hydroxyethyl)-4-bromo-5,6,7,8-tetrahydronaphthyl-3-carboxylate (18). To a solution of 9-BBN dimer (3.1 g, 12.8 mmol)

in THF (80 mL) was added a solution of **17** (5.3 g, 17.1 mmol) in THF (20 mL). After stirring for 16 h, the solution was cooled to −30 °C and treated with 30% H_2O_2 (4.3 mL, 40.0 mmol) followed by 3 N NaOH (13.3 mL, 40.0 mmol). The mixture was warmed to 0−10 °C and stirred for 3 h, diluted with water, and extracted with ether. The combined extracts were washed with water and brine, dried ($MgSO_4$), and evaporated. The residue was purified by chromatography (30% EtOAc in hexane) to give 3.2 g (57%) of **18** as an oil: ^{1}H NMR (DMSO-d_6) δ 1.31 (t, 3H, J = 7 Hz), 1.73 (m, 4H), 2.6−2.9 (m, 6H), 3.6 (q, 2H, J = 5 Hz, collapsible to t with D_2O), 4.32 (q, 2H, J = 7 Hz), 4.7 (t, 1H, J = 5 Hz, collapsible with D_2O), 7.27 (s, 1H).

Ethyl 1-(2-Bromoethyl)-4-bromo-5,6,7,8-tetrahydronaphthyl-3-carboxylate (19). To a 0 °C solution of **18** (3.2 g, 9.7 mmol) in dry CH_2Cl_2 (60 mL) was added triphenylphosphine (3.8 g, 14.6 mmol) followed by carbon tetrabromide (4.8 g, 14.6 mmol). After the resulting mixture was stirred for 1 h, the solvent was evaporated and the residue purified by chromatography (5% EtOAc in hexane) to give 2.9 g (76%) of **19** as an oil: ^{1}H NMR (DMSO-d_6) δ 1.31 (t, 3H, J = 7 Hz), 1.7 (m, 4H), 2.7 (m, 4H), 3.1 (t, 2H, J = 7 Hz), 3.69 (t, 2H, J = 7 Hz), 4.32 (q, 2H, J = 7 Hz), 7.3 (s, 1H).

3-[2-(3-Carboxy-4-bromo-5,6,7,8-tetrahydronaphthyl)ethyl]coformycin Aglycon (14). 14 was prepared from compound **19** and ketone **7** by using the procedures described for compounds **9** and **10**. mp >200 °C dec; ^{1}H NMR (DMSO-d_6) δ 1.69 (m, 4H), 2.65 (m, 4H), 2.85 (t, 2H, J = 7 Hz), 3.18 (br s, 2H), 4.0 (t, 2H, J = 7 Hz), 4.8 (br s, 1H), 4.95 (br s, 1H), 6.86 (s, 1H), 7.0 (d, 1H, J = 4 Hz), 7.27 (s, 1H), 7.5 (br s, 1H). Anal. Calcd for $C_{19}H_{21}N_4O_3Br\cdot 2.5H_2O\cdot 1.2CH_3CO_2H$: C, 46.70; H, 5.59; N, 10.18. Found: C, 46.13; H, 4.94; N, 10.17.

3,6,7,8-Tetrahydroimidazo[4,5-*d*]-[1,3]diazepine Hydrochloride (21). A mixture of 4(5)-nitrohistamine hydrochloride salt **20**[38] (4.36 g, 22.6 mmol), triethyl orthoformate (150 mL), and 10% Pd/C (3.3 g) in EtOH (200 mL) was stirred under 1 atm H_2 at rt. After 2 h, the reaction mixture was warmed to 50 °C and stirred 4 h and then warmed to 70 °C for 48 h. The solvent and excess triethyl orthoformate were removed under reduced pressure. The resulting dark hygroscopic solid was triturated with EtOH to give 1.25 g (32%) of **21** as a brown solid: ^{1}H NMR (DMSO-d_6) δ 3.01 (t, 2H, J = 4.3 Hz), 3.6 (m, 2H), 7.57 (s, 1H) 7.87 (d, 1H, J = 6.9 Hz), 10.2 (br s, 1H); MS (ES) m/z 137 (MH^+).

3-[2-(3-Carboxy-4-bromo-5,6,7,8-tetrahydronaphthyl)ethyl]-3,6,7,8-tetrahydroimidazo[4,5-*d*]-[1,3]diazepine Dicyclohexylammonium Salt (22). Compound **21** was free-based as described for compound **7** and alkylated with **23**[39] as described for the preparation of **9**. The resulting benzyl ester (110 mg, 0.22 mmol) was subjected to hydrogenolysis by stirring with dicyclohexylamine (77 mg, 0.44 mmol) and 30 mg of 10% Pd/C in MeOH (20 mL) under 1 atm H_2. After 16 h, the solvent was removed under reduced pressure and the residue triturated with ether to give 80 mg of **22**[40] as light yellow solid: ^{1}H NMR (D_2O) δ 1.0−2.1 (series of m, 24H), 2.3 (t, 2H, J = 6 Hz), 2.6 (t, 2H, J = 6 Hz), 2.8 (t, 2H, J = 4 Hz), 2.9 (t, 2H, J = 6 Hz), 3.0−3.3 (m, 2H), 3.3 (t, 2H, J = 4 Hz), 4.1 (t, 2H, J = 6 Hz), 6.7 (s, 1H), 6.92 (s, 1H), 6.96 (s, 1H); MS (ES) m/z 418 (MH^+).

ADA Binding Conformation of 8. The X-ray structure of murine adenosine deaminase complexed with (6*R*)-6-hydroxy-1,6-dihydropurine riboside (**3**) (pdb file name: 2ADA) provided the initial atomic coordinates used to generate the computer model[29] and conduct the energy calculations. Compound **8** was docked in the ADA active site by superpositioning the base with the base of **3** and applying the previously described atomic constraints. The torsion angle for each rotatable bond was randomly varied between 0 and 360 degrees using the Monte Carlo (MC) search method within the MacroModel program. All conformations generated (500) were subjected to a short (100-step) energy minimization procedure by using the conjugate gradient minimizer and the AMBER force field. Conformations were compared for uniqueness relative to previously generated conformations. The five lowest energy conformations were selected and further minimized using the all-atom force field of AMBER.

Conformational Analysis of 13. Low energy conformations of **13** were identified following gas-phase energy minimization of conformations generated by using the MC conformational search method.

Adenosine Monophosphate Deaminase. Porcine heart AMPDA was purified essentially as described by Smiley et al. through the phosphocellulose step.[48] Inhibition of AMPDA activity was determined at 37 °C in a 0.1-mL assay mixture containing inhibitor, ∼0.005 units of porcine heart or recombinant human E-type AMPDA, 0.1% bovine serum albumin, 10 mM ATP, 250 mM KCl, and 50 mM MOPS at pH 6.5. The concentration of the substrate AMP was varied from 0.125 to 10.0 mM. The reaction was initiated by the addition of AMPDA to the otherwise complete reaction mixture and terminated after 5 min by injection into an HPLC system. Activities were determined from the amount of IMP formed over 5 min. IMP was separated from AMP by HPLC using a Beckman Ultrasil-SAX anion-exchange column (4.6 mm × 25 cm) with an isocratic buffer system (12.5 mM potassium phosphate, 30 mM KCl, pH 3.5) and detected spectrophotometrically at 254 nm.

Adenosine Deaminase. Inhibition of ADA from calf intestinal mucosa was determined spectrophotometrically at pH 7.0 and 37 °C. The reaction mixture (1 mL) contained inhibitor, 0.001 units ADA, and 40 mM potassium phosphate. The concentration of adenosine was varied from 20 to 100 μM. The reaction was initiated by addition of ADA and monitored continuously at 265 nm for 15 min. Decreases in absorbance reflected conversion of adenosine to inosine.

Hepatocyte Uptake Studies. Isolated rat hepatocytes were prepared from fed rats by the collagenase digestion technique.[49] Cells were suspended at a density of 75 mg wet weight/ml of Krebs bicarbonate buffer supplemented with 10 mM glucose. Incubations were performed in sealed plastic tubes under a 95% oxygen/5% carbon dioxide atmosphere. The tubes were kept at 37 °C and continuously agitated in a shaking water bath. Cells were given a 15 min equilibration period prior to the start of an experiment. Typical energy charges of cell preparations ranged from 0.8 to 0.85, while ATP concentrations ranged from 1.8 to 2.4 μmol/g of cells. These values are comparable to those measured in freeze-clamped rat liver biopsies [0.81 ± 0.03 and 2.21 ± 0.4 for energy charge and ATP content, respectively]. Cells were incubated with AMPDA inhibitors at the indicated concentrations, and aliquots were removed at the specified time intervals over the course of 1 h. The removal of extracellular drug, and the extraction of cells was achieved by centrifugation of the aliquots through an oil layer into 10% perchloric acid. The acid layer was neutralized, clarified, and analyzed for drug content by HPLC. A C_{18} reverse phase column and an acetonitrile gradient were used to identify and quantify peaks relative to known standards.

Nucleotide Determinations in Rat Hepatocytes Subjected to Fructose or Anoxia. Isolated rat hepatocytes were incubated in the presence of vehicle or an AMPDA inhibitor for 5 min. Cellular stress was induced by the addition of fructose (0.5 mg/mL) to the cell medium as described by Woods et al.[50] or by subjecting the cells to 15 min of anoxia by replacement of the gaseous phase with a 95% nitrogen/5% carbon dioxide gas mixture. At appropriate time intervals prior to and after stress induction, aliquots of the cell suspensions were removed, and the cells were extracted by acidification with perchloric acid. After neutralization and clarification of the cell extracts, nucleotide content was determined by HPLC. Separation of nucleotides was performed on an anion-exchange column eluted with a potassium phosphate/potassium chloride gradient. Identification and quantitation of nucleotides was achieved by comparison to the elution profile and peak areas of authentic standards (Sigma, St. Louis, MO) of known concentration. Statistical analysis was performed with the unpaired Student's t test. A value of $p < 0.05$ was considered statistically significant.

Adenosine Determinations in Rat Hepatocytes Subjected to Fructose or Anoxia. The experimental conditions described above were also used in studies evaluating the effect of drug treatment on total adenosine. Adenosine levels were quantitated by reverse phase HPLC. In some instances, generation of adenosine was confirmed by its conversion to ethenoadenosine with chloroacetaldehyde. By using the oil-separation technique described above, the amount of adenosine secreted into the cell medium was determined. The concentration

(48) Smiley, K. L., Jr.; Berry, A. J.; Suelter, C. H. *J. Biol. Chem.* **1967**, *242*, 2502−2506.
(49) Berry, M. N.; Friend, D. S. *J. Cell. Biol.* **1969**, *43*, 506−520.
(50) Woods, H. F. *Biochem. J.* **1970**, *119*, 501−510.

required to elicit a half-maximal increase in total adenosine levels 10 min post-fructose exposure was defined as the ED_{50}.

Acknowledgment. We thank Mr. Gary Probst, Ms. Wei Xiao, Ms. Maureen Cottrell, Dr. Christen Anderson, Mr. Colin Ingraham, Mr. Patrick McCurley, Dr. William Sun, and Dr. Ken Takabayashi for their scientific contributions to this work. We would also like to thank Ms. Lisa Weston for her assistance in preparing this manuscript.

Supporting Information Available: Experimental procedures and data for ethyl 2-(phenylmethyl)-6-methanesulfonoxyhexonate and 4-propoxyphenylpropyl methanesulfonate. Assay procedures for phosphofructokinase, fructose 1,6-bisphosphatase, glycogen phosphorylase, adenylate kinase and adenosine kinase (5 pages, print/PDF). See any current masthead page for ordering information and Web access instructions.

JA983153J